Fatigue Failure of Development Space Shuttle Main Engine Turbine Blades

SSME POWERHEAD

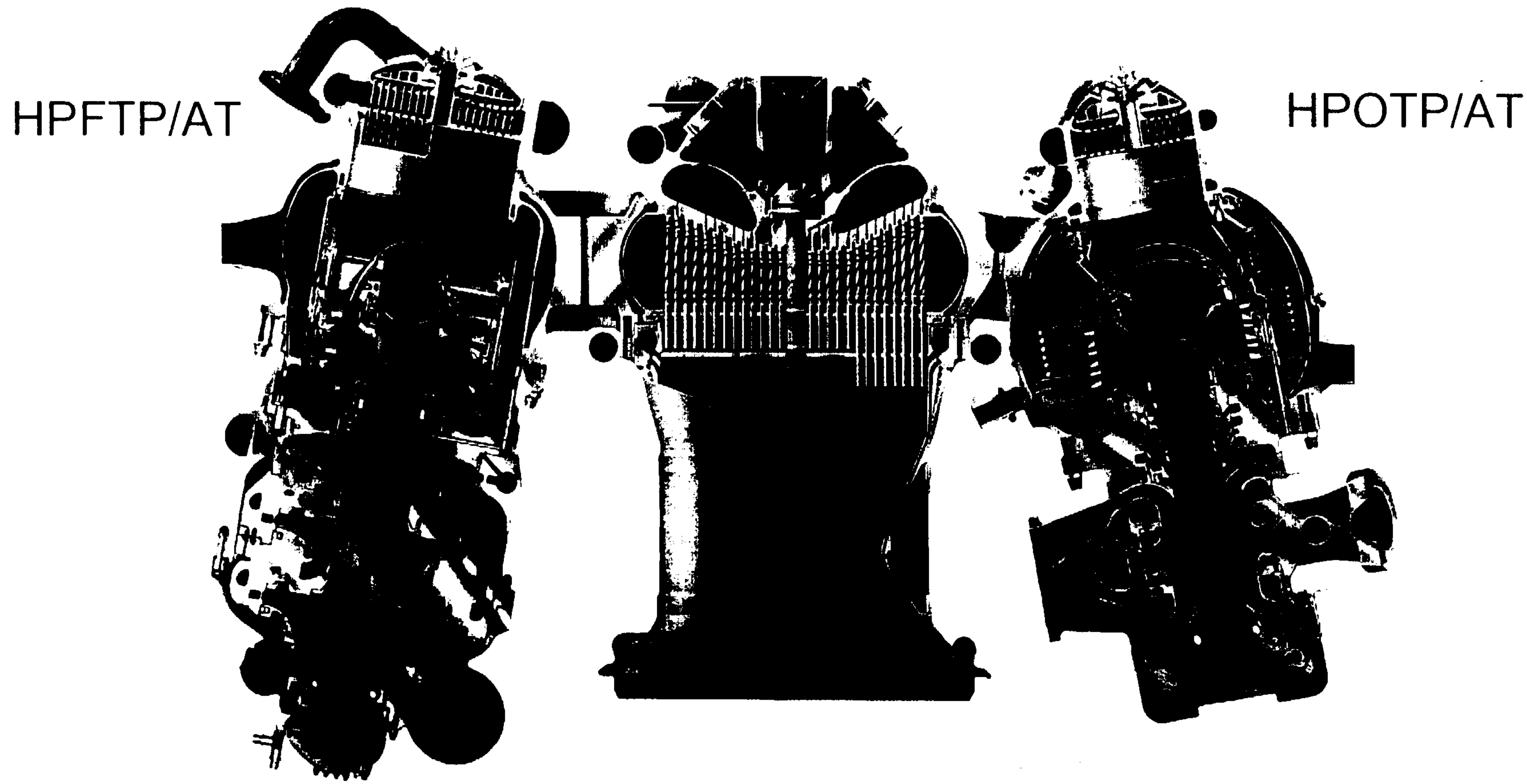

HPFTP/AT

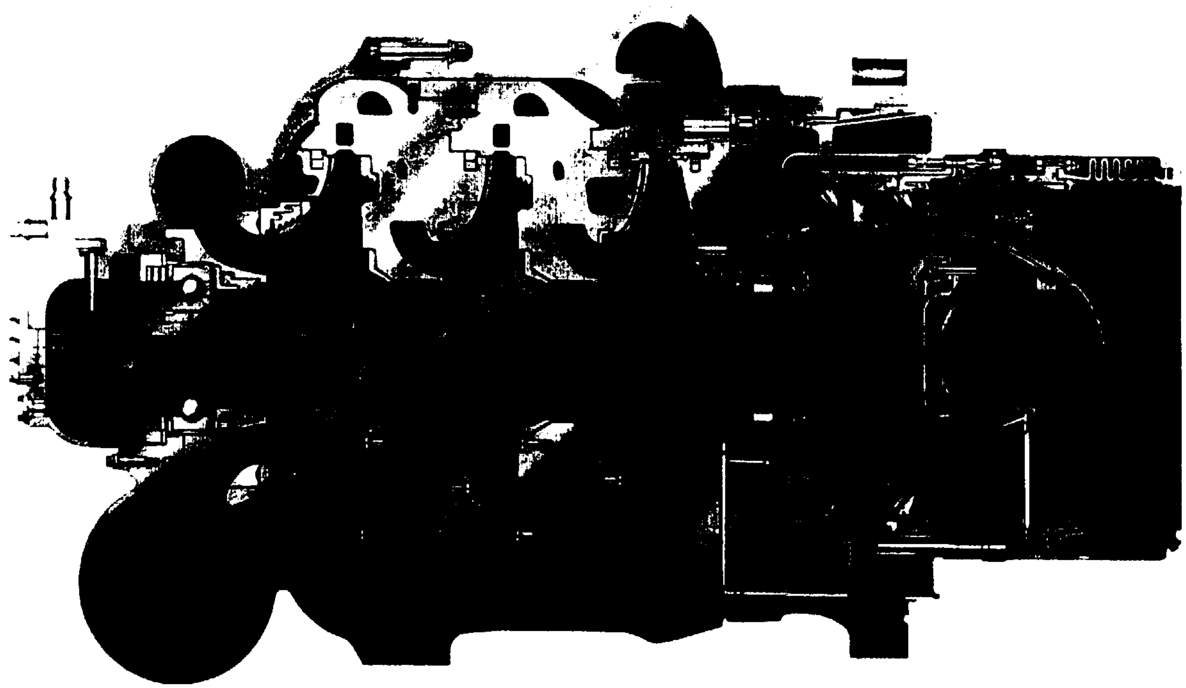

Fatigue Failure of Development Space Shuttle Main Engine Turbine Blades

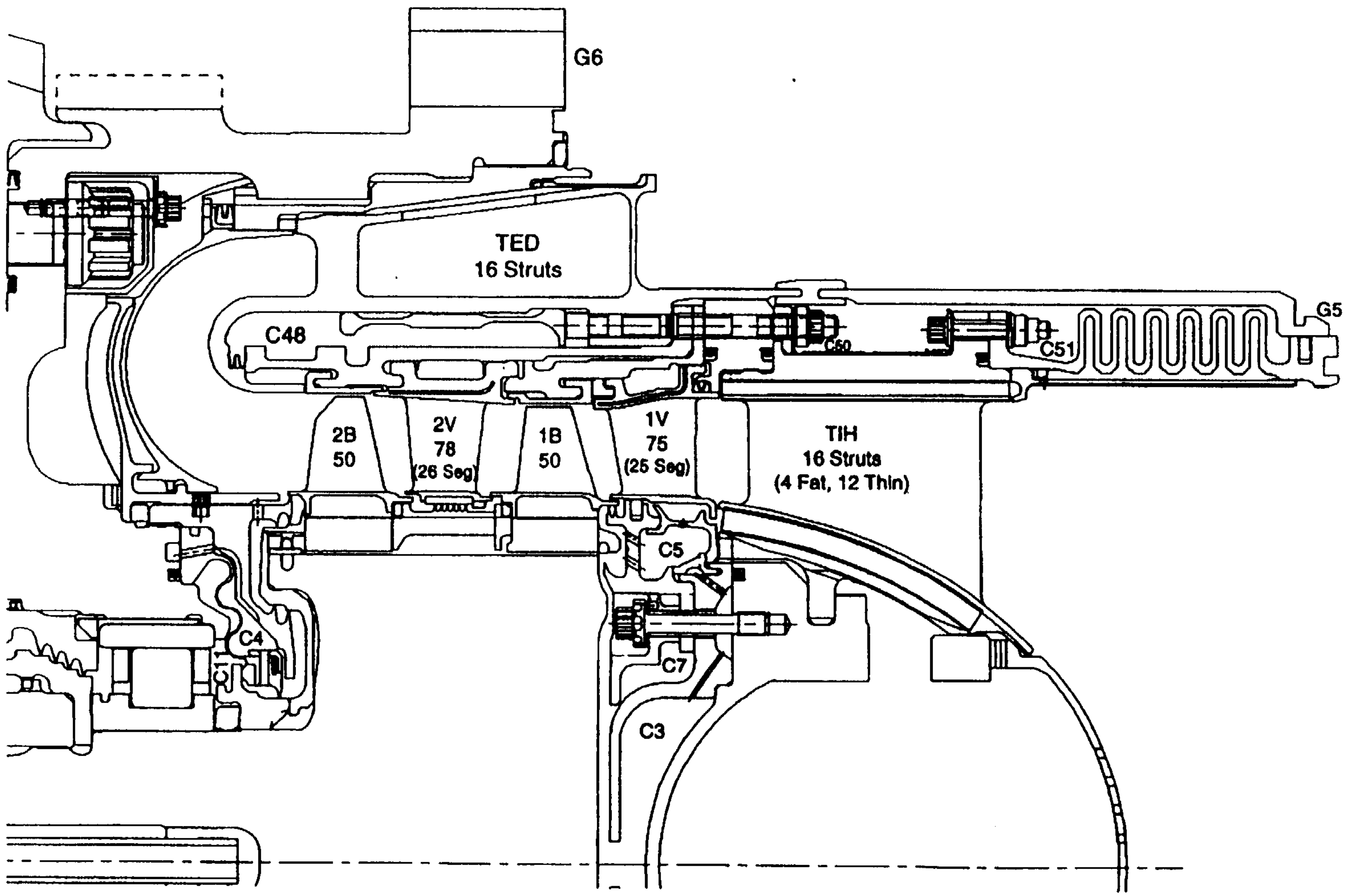

Agenda

- Single Crystal Material
- Uniaxial LCF Specimen Data
- Development Blade Failure Analysis

Single Crystal Materials

- **Anisotropic Material**
  - Nickel based (face centered cubic structure)
  - Properties vary with orientation
  - Contains preferential easy slip systems

- **No Grain Boundaries**
  - Higher strength at elevated temperature
  - Greater creep resistance at elevated temperature

- **Possible to Control Crystal Orientation Within A Structure**
  - P&W controls the primary material axis to within 15 degrees of the stacking axis
  - The secondary axis is uncontrolled

Coordinate Transformations for Orthotropic Material

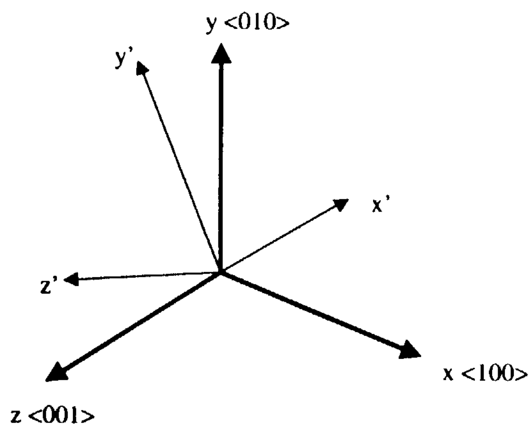

<u>Hooke's Law</u>
$\{\sigma\} = [D]\{\varepsilon\}$
$\{\sigma'\} = [D']\{\varepsilon'\}$
$[D'] = [Q]^T [D] [Q]$

$[Q] = (6x6)$ matrix of direction cosines

Single crystal material can be thought of as a 3D composite. The material properties are orthotropic and vary with orientation. Orthotropic materials with cubic symmetry have 3 independent material properties: E, ν, and G.

$$\{\sigma'\} = [Q']\{\sigma\}$$

$$\{\sigma\} = [Q']^{-1}\{\sigma'\} = [Q]\{\sigma'\}$$

$$\{\varepsilon'\} = [Q'_\varepsilon]\{\varepsilon\}$$

$$\{\varepsilon\} = [a_{ij}]\{\sigma\}$$

$$a_{11} = \frac{1}{E_{xx}},\ a_{44} = \frac{1}{G_{yz}},\ a_{12} = -\frac{\nu_{yx}}{E_{xx}} = -\frac{\nu_{xy}}{E_{yy}}$$

$$\{\varepsilon\} = [a_{ij}]\{\sigma\} \qquad \{\varepsilon'\} = [a'_{ij}]\{\sigma'\}$$

$$[a'_{ij}] = [Q]^T [a_{ij}][Q] = \sum_{m=1}^{6}\sum_{n=1}^{6} a_{mn} Q_{mi} Q_{nj}$$

$$(i, j = 1, 2, \ldots\ldots, 6)$$

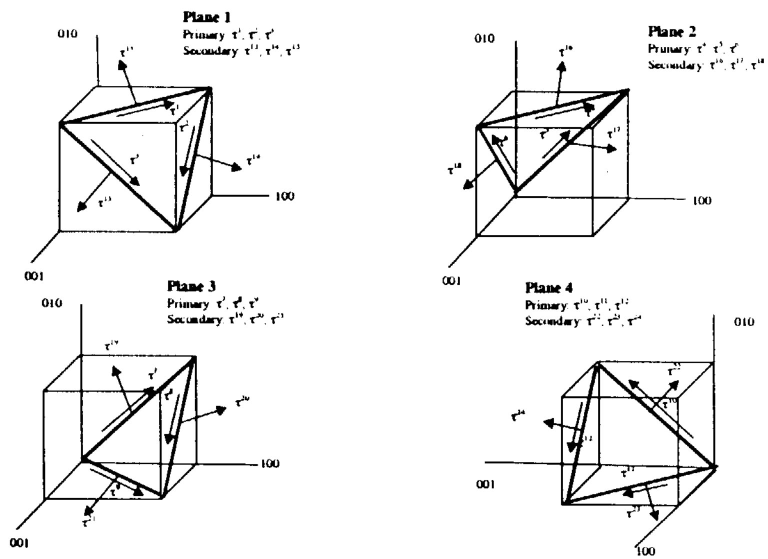

Fig. 3.1 Primary (close-pack) and secondary (non-close-pack) slip directions on the octahedral planes for a FCC crystal [4]

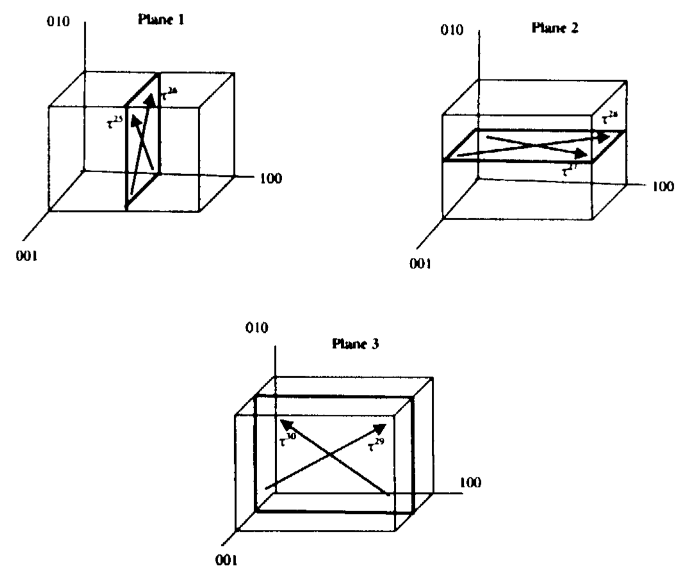

Fig. 3.2 Cube slip planes and slip directions for a FCC crystal [4]

$$\begin{Bmatrix} \tau^{1} \\ \tau^{2} \\ \tau^{3} \\ \tau^{4} \\ \tau^{5} \\ \tau^{6} \\ \tau^{7} \\ \tau^{8} \\ \tau^{9} \\ \tau^{10} \\ \tau^{11} \\ \tau^{12} \end{Bmatrix} = \frac{1}{\sqrt{6}} \begin{bmatrix} 1 & 0 & -1 & 1 & 0 & -1 \\ 0 & -1 & 1 & -1 & 1 & 0 \\ 1 & -1 & 0 & 0 & 1 & -1 \\ -1 & 0 & 1 & 1 & 0 & -1 \\ -1 & 1 & 0 & 0 & -1 & -1 \\ 0 & 1 & -1 & -1 & -1 & 0 \\ 1 & -1 & 0 & 0 & -1 & -1 \\ 0 & 1 & -1 & -1 & 1 & 0 \\ 1 & 0 & -1 & -1 & 0 & -1 \\ 0 & -1 & 1 & -1 & -1 & 0 \\ -1 & 0 & 1 & -1 & 0 & -1 \\ -1 & 1 & 0 & 0 & 1 & -1 \end{bmatrix} \begin{Bmatrix} \sigma_{xx} \\ \sigma_{yy} \\ \sigma_{zz} \\ \sigma_{xy} \\ \sigma_{zx} \\ \sigma_{yz} \end{Bmatrix}$$

$$\begin{Bmatrix} \tau^{13} \\ \tau^{14} \\ \tau^{15} \\ \tau^{16} \\ \tau^{17} \\ \tau^{18} \\ \tau^{19} \\ \tau^{20} \\ \tau^{21} \\ \tau^{22} \\ \tau^{23} \\ \tau^{24} \end{Bmatrix} = \frac{1}{3\sqrt{2}} \begin{bmatrix} -1 & 2 & -1 & 1 & -2 & 1 \\ 2 & -1 & -1 & 1 & 1 & -2 \\ -1 & -1 & 2 & -2 & 1 & 1 \\ -1 & 2 & -1 & -1 & -2 & -1 \\ -1 & -1 & 2 & 2 & 1 & -1 \\ 2 & -1 & -1 & -1 & 1 & 2 \\ -1 & -1 & 2 & 2 & -1 & 1 \\ 2 & -1 & -1 & -1 & -1 & -2 \\ -1 & 2 & -1 & -1 & 2 & 1 \\ 2 & -1 & -1 & 1 & -1 & 2 \\ -1 & 2 & -1 & 1 & 2 & -1 \\ -1 & -1 & 2 & -2 & -1 & -1 \end{bmatrix} \begin{Bmatrix} \sigma_{xx} \\ \sigma_{yy} \\ \sigma_{zz} \\ \sigma_{xy} \\ \sigma_{zx} \\ \sigma_{yz} \end{Bmatrix}$$

$$\begin{Bmatrix} \tau^{25} \\ \tau^{26} \\ \tau^{27} \\ \tau^{28} \\ \tau^{29} \\ \tau^{30} \end{Bmatrix} = \frac{1}{\sqrt{2}} \begin{bmatrix} 0 & 0 & 0 & 1 & 1 & 0 \\ 0 & 0 & 0 & 1 & -1 & 0 \\ 0 & 0 & 0 & 1 & 0 & 1 \\ 0 & 0 & 0 & 1 & 0 & -1 \\ 0 & 0 & 0 & 0 & 1 & 1 \\ 0 & 0 & 0 & 0 & -1 & 1 \end{bmatrix} \begin{Bmatrix} \sigma_{xx} \\ \sigma_{yy} \\ \sigma_{zz} \\ \sigma_{xy} \\ \sigma_{zx} \\ \sigma_{yz} \end{Bmatrix}$$

Resolved shear stresses from the material coordinate system stress tensor

$$\begin{Bmatrix} \gamma^{1} \\ \gamma^{2} \\ \gamma^{3} \\ \gamma^{4} \\ \gamma^{5} \\ \gamma^{6} \\ \gamma^{7} \\ \gamma^{8} \\ \gamma^{9} \\ \gamma^{10} \\ \gamma^{11} \\ \gamma^{12} \end{Bmatrix} = \frac{2}{\sqrt{6}} \begin{bmatrix} 1 & 0 & -1 & 1 & 0 & -1 \\ 0 & -1 & 1 & -1 & 1 & 0 \\ 1 & -1 & 0 & 0 & 1 & -1 \\ -1 & 0 & 1 & 1 & 0 & -1 \\ -1 & 1 & 0 & 0 & -1 & -1 \\ 0 & 1 & -1 & -1 & -1 & 0 \\ 1 & -1 & 0 & 0 & -1 & -1 \\ 0 & 1 & -1 & -1 & 1 & 0 \\ 1 & 0 & -1 & -1 & 0 & -1 \\ 0 & -1 & 1 & -1 & -1 & 0 \\ -1 & 0 & 1 & -1 & 0 & -1 \\ -1 & 1 & 0 & 0 & 1 & -1 \end{bmatrix} \begin{Bmatrix} \varepsilon_{xx} \\ \varepsilon_{yy} \\ \varepsilon_{zz} \\ \varepsilon_{xy} \\ \varepsilon_{zx} \\ \varepsilon_{yz} \end{Bmatrix}$$

$$\begin{Bmatrix} \gamma^{13} \\ \gamma^{14} \\ \gamma^{15} \\ \gamma^{16} \\ \gamma^{17} \\ \gamma^{18} \\ \gamma^{19} \\ \gamma^{20} \\ \gamma^{21} \\ \gamma^{22} \\ \gamma^{23} \\ \gamma^{24} \end{Bmatrix} = \frac{2}{3\sqrt{2}} \begin{bmatrix} -1 & 2 & -1 & 1 & -2 & 1 \\ 2 & -1 & -1 & 1 & 1 & -2 \\ -1 & -1 & 2 & -2 & 1 & 1 \\ -1 & 2 & -1 & -1 & -2 & -1 \\ -1 & -1 & 2 & 2 & 1 & -1 \\ 2 & -1 & -1 & -1 & 1 & 2 \\ -1 & -1 & 2 & 2 & -1 & 1 \\ 2 & -1 & -1 & -1 & -1 & -2 \\ -1 & 2 & -1 & -1 & 2 & 1 \\ 2 & -1 & -1 & 1 & -1 & 2 \\ -1 & 2 & -1 & 1 & 2 & -1 \\ -1 & -1 & 2 & -2 & -1 & -1 \end{bmatrix} \begin{Bmatrix} \varepsilon_{xx} \\ \varepsilon_{yy} \\ \varepsilon_{zz} \\ \varepsilon_{xy} \\ \varepsilon_{zx} \\ \varepsilon_{yz} \end{Bmatrix}$$

$$\begin{Bmatrix} \gamma^{25} \\ \gamma^{26} \\ \gamma^{27} \\ \gamma^{28} \\ \gamma^{29} \\ \gamma^{30} \end{Bmatrix} = \frac{2}{\sqrt{2}} \begin{bmatrix} 0 & 0 & 0 & 1 & 1 & 0 \\ 0 & 0 & 0 & 1 & -1 & 0 \\ 0 & 0 & 0 & 1 & 0 & 1 \\ 0 & 0 & 0 & 1 & 0 & -1 \\ 0 & 0 & 0 & 0 & 1 & 1 \\ 0 & 0 & 0 & 0 & -1 & 1 \end{bmatrix} \begin{Bmatrix} \varepsilon_{xx} \\ \varepsilon_{yy} \\ \varepsilon_{zz} \\ \varepsilon_{xy} \\ \varepsilon_{zx} \\ \varepsilon_{yz} \end{Bmatrix}$$

Resolved engineering shear strains from the material coordinate system strain tensor

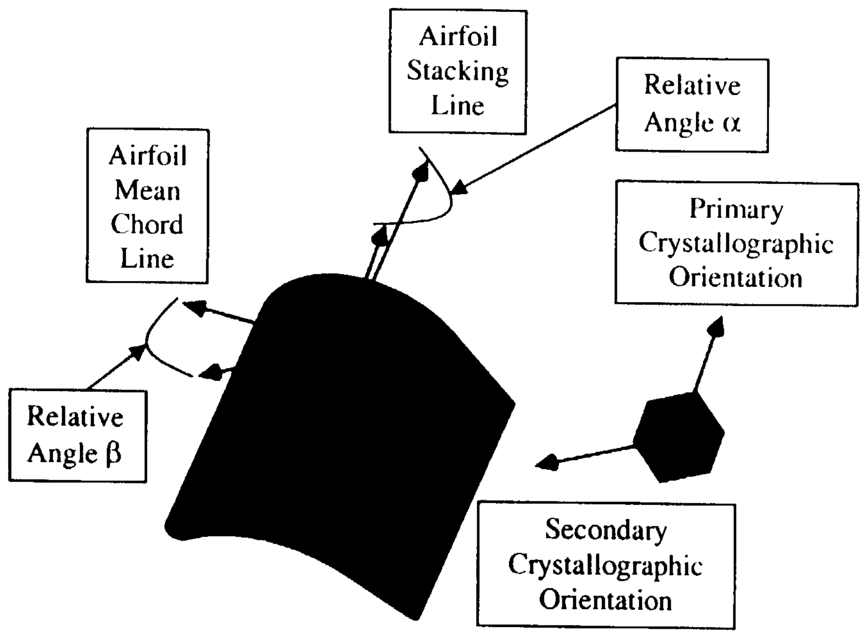

Fig. 2.4 Convention for Defining Crystal Orientation in Turbine Blades[2]

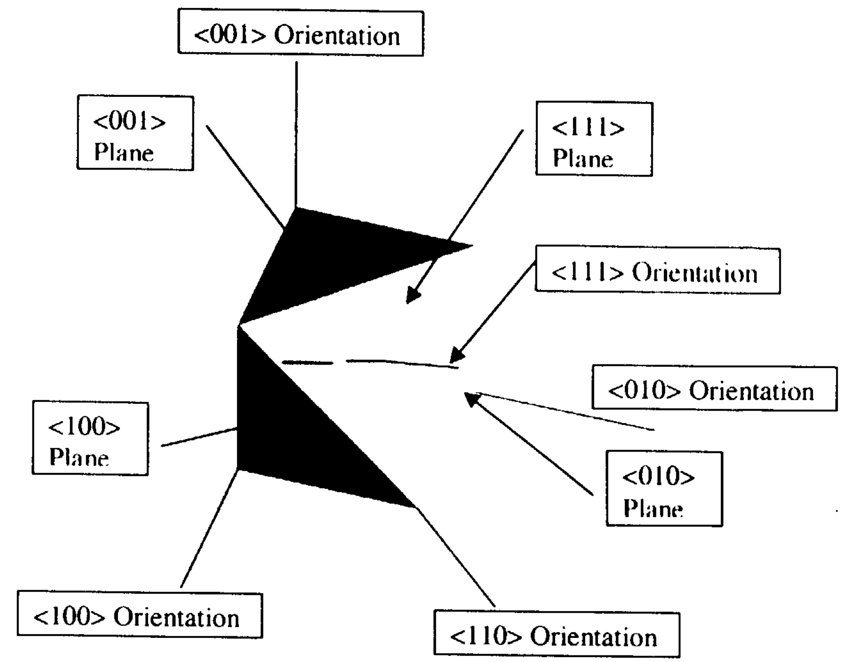

Fig. 2.3 FCC Crystallographic Orientation[2]

Fatigue Failure of Development Space Shuttle Main Engine Turbine Blades

Single Crystal Cracks

- Crack is on crystal <111> family of planes

Fig. 3.3 A subsurface fretting fatigue crack emanating from a carbide in a turbine blade attachment (PWA1422) and propagating along octahedral (111) shear planes[1].

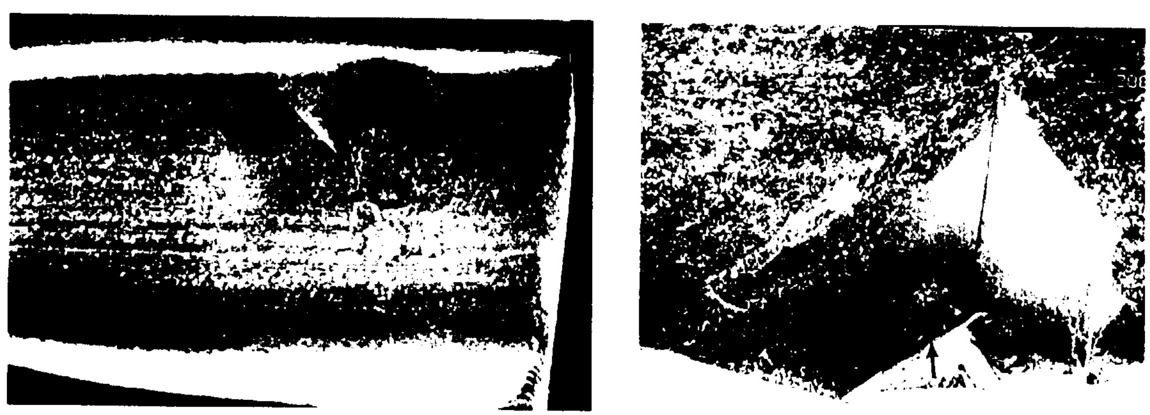

Fig. 3.4 Subsurface fretting fatigue crystallographic crack initiation in a single crystal Ni turbine blade platform[5]

Fatigue Failure of Development Space Shuttle Main Engine Turbine Blades

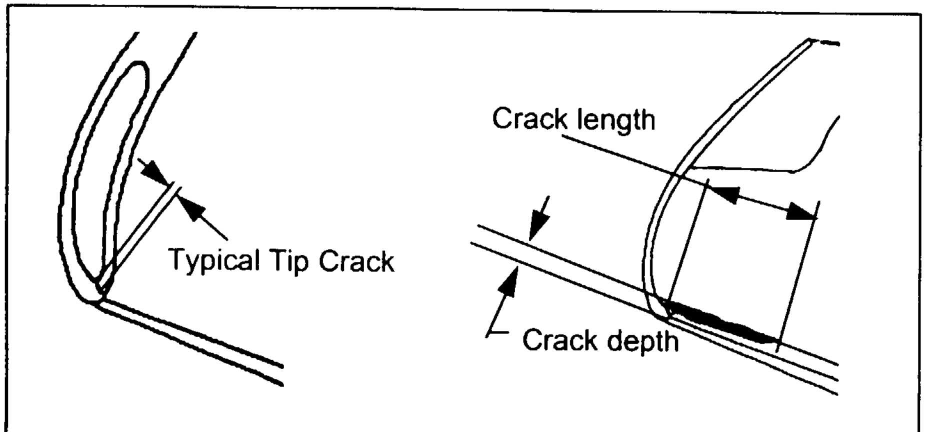

Blade leading edge crack location and orientation

Development Blade Crack Locations

- Tip initiation at core leading edge (resolved for certification and flight by increasing core radius)
- Attachment at galling location (resolved for certification and flight by reducing attachment temperature, and by gold plating blade to reduce friction)

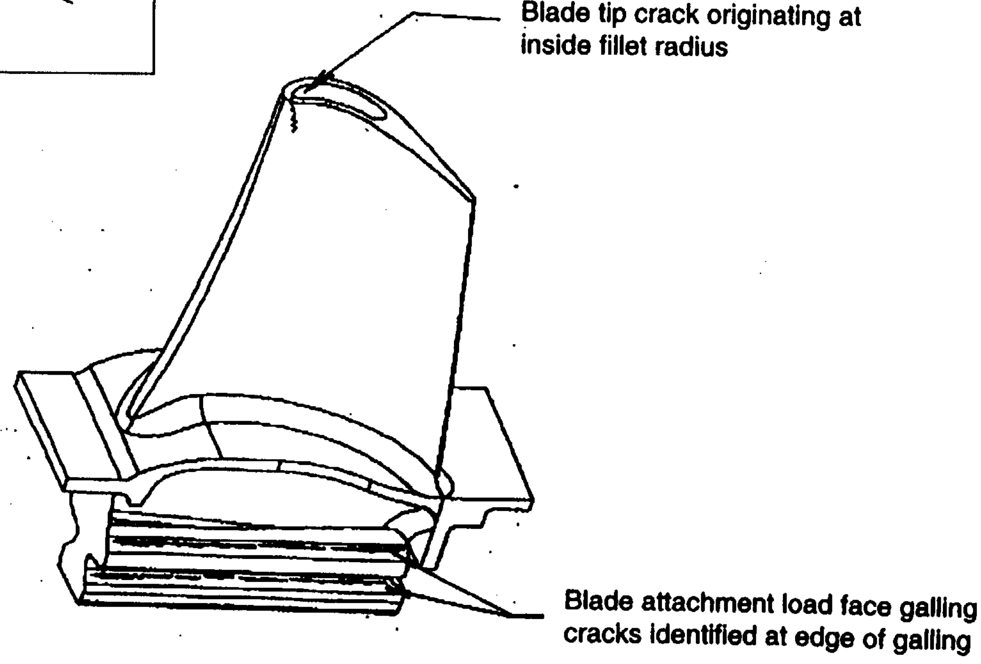

1st Turbine Blade

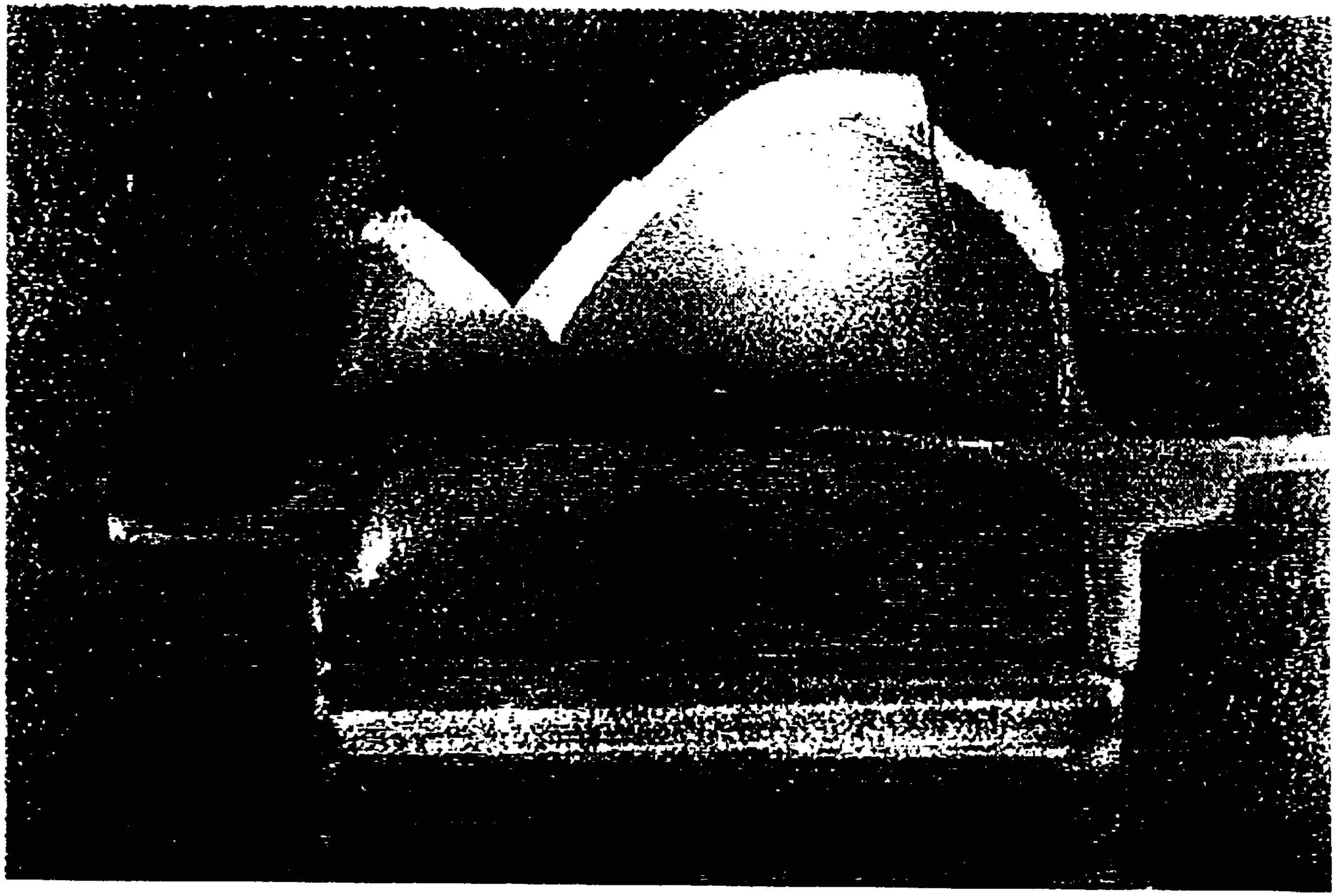

Development Blade Airfoil Failure

Power Law Curve Fit (<u>R^2 = 0.468</u>): $\Delta\varepsilon = \mathbf{0.0238\ N^{-0.124}}$

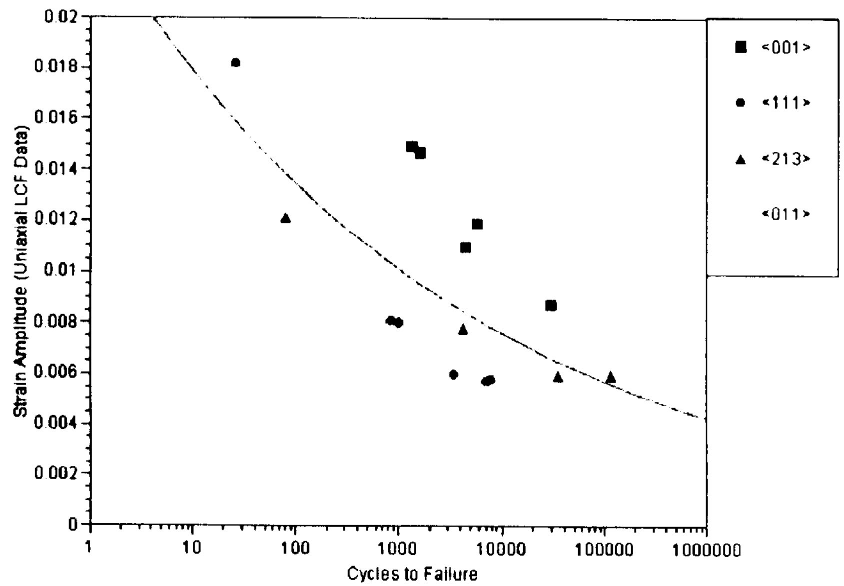

Fig. 4.3 Strain range Vs. Cycles to Failure for LCF test data (PWA1484 at 1200F)

Power Law Curve Fit (<u>R^2 = 0.674</u>): $\Delta\tau = \mathbf{397{,}758\ N^{-0.1598}}$

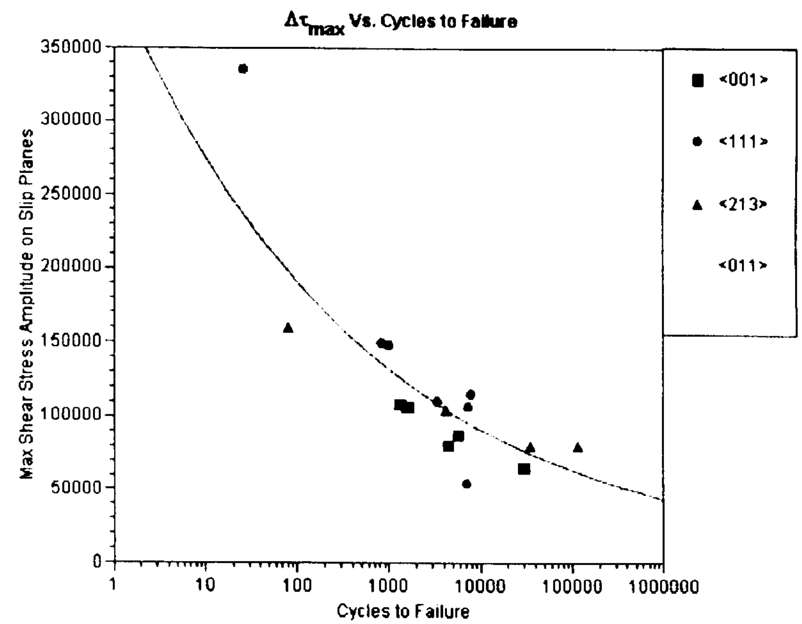

Fig. 4.8 Shear Stress Amplitude [$\Delta\tau_{max}$] Vs. N

Fatigue Failure of Development Space Shuttle Main Engine Turbine Blades

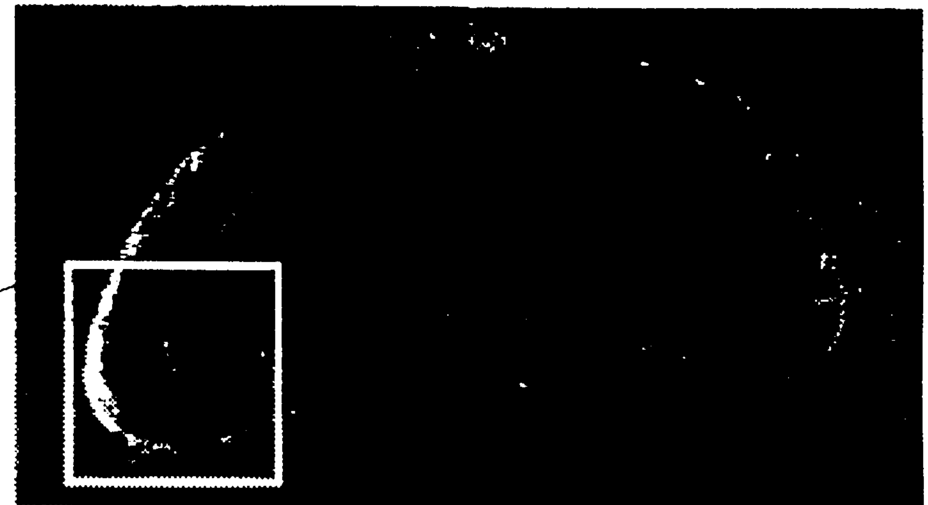

Development Blade Core Profile

- Sharp reentrant corner
- Wall thickness variation
- Resolved for certification and flight by increasing core radius and tighter control of core placement

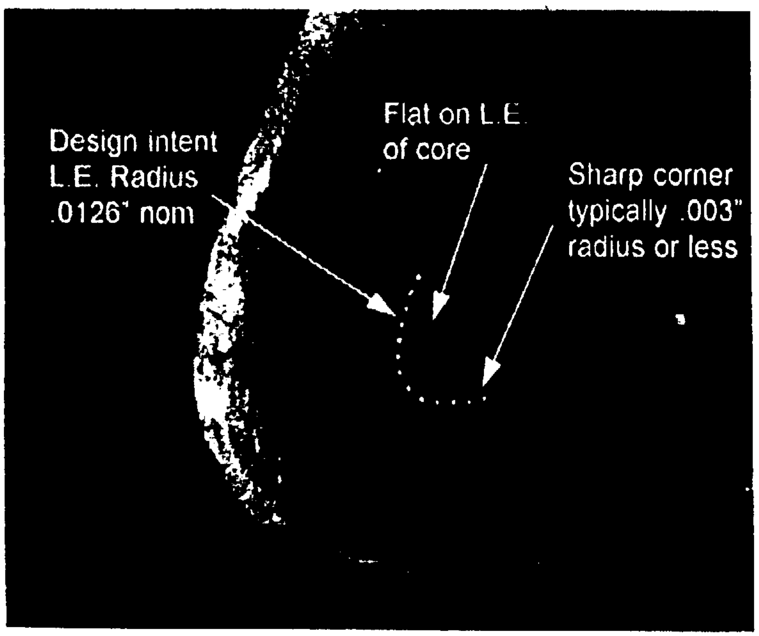

Correlation Coefficient, R^2	Power Law Curve Fit
0.468	Strain Range, $\Delta\varepsilon = 0.0238\ N^{-0.124}$
0.130	$[\gamma_{max} + \varepsilon_n] = 0.0249\ N^{-0.773}$
0.391	$\left[\frac{\Delta\gamma}{2} + \frac{\Delta\varepsilon_n}{2} + \frac{\sigma_{no}}{E}\right] = 0.0206\ N^{-0.101}$
0.383	$\left[\frac{\Delta\gamma}{2}\left(1 + k\frac{\sigma_n^{max}}{\sigma_y}\right)\right] = 0.0342\ N^{-0.143}$
0.189	$\left[\frac{\Delta\varepsilon_1}{2}(\sigma^{max})\right] = 334.6\ N^{-0.209}$
0.674	$\Delta\tau_{max} = 397{,}758\ N^{-0.1598}$ (Max shear stress amplitude of 30 slip systems)
0.744	$\Delta\tau_{max} * \Delta\gamma/2 = 2{,}641\ N^{-0.256}$
0.549	$\tau_{max} * \Delta\gamma/2 = 4{,}661\ N^{-0.227}$
0.775	$\Delta\sigma_{vonMises} = 845{,}607\ N^{-0.157}$ [Equivalent stress (von Mises) amplitude]
0.775	$\Delta\tau_{Tresca} = 422{,}946\ N^{-0.157}$ (Max principal shear stress amplitude)

Table 4.6 Power law curve fits for the failure parameters

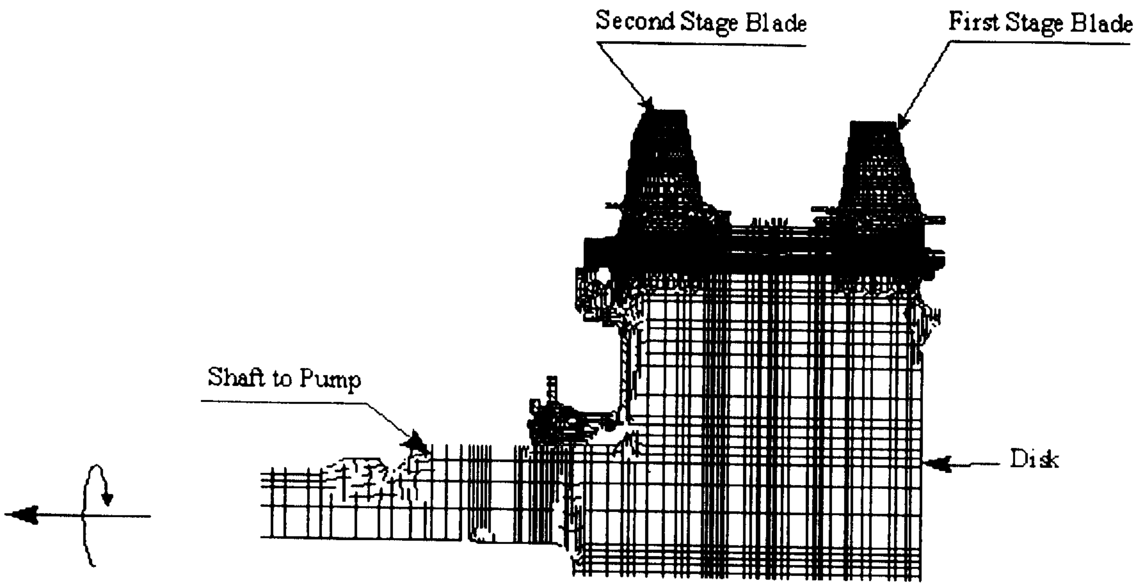

Figure 27. 3D ANSYS model of HPFTP/AT rotating turbine components.

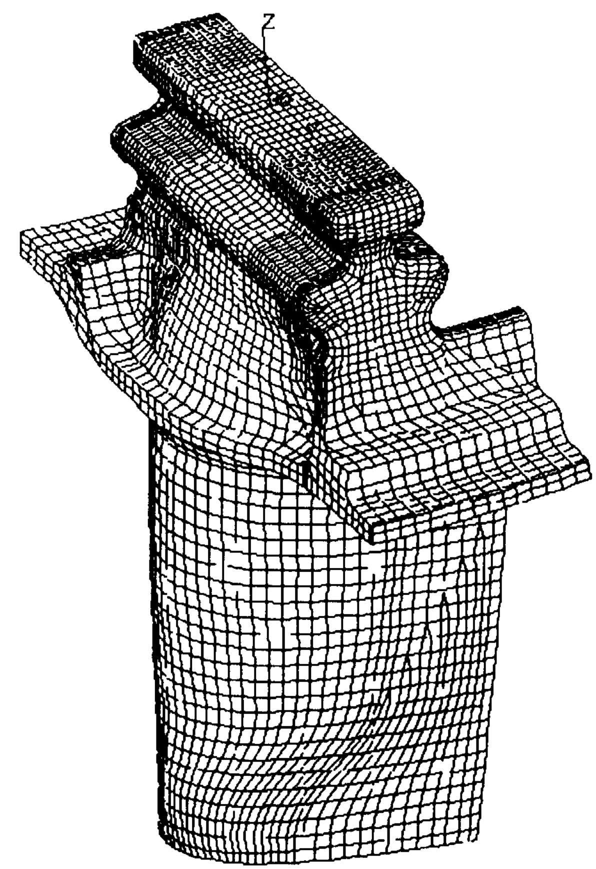

Figure 28. First Stage Blade Casting Coordinate System

Fatigue Failure of Development Space Shuttle Main Engine Turbine Blades

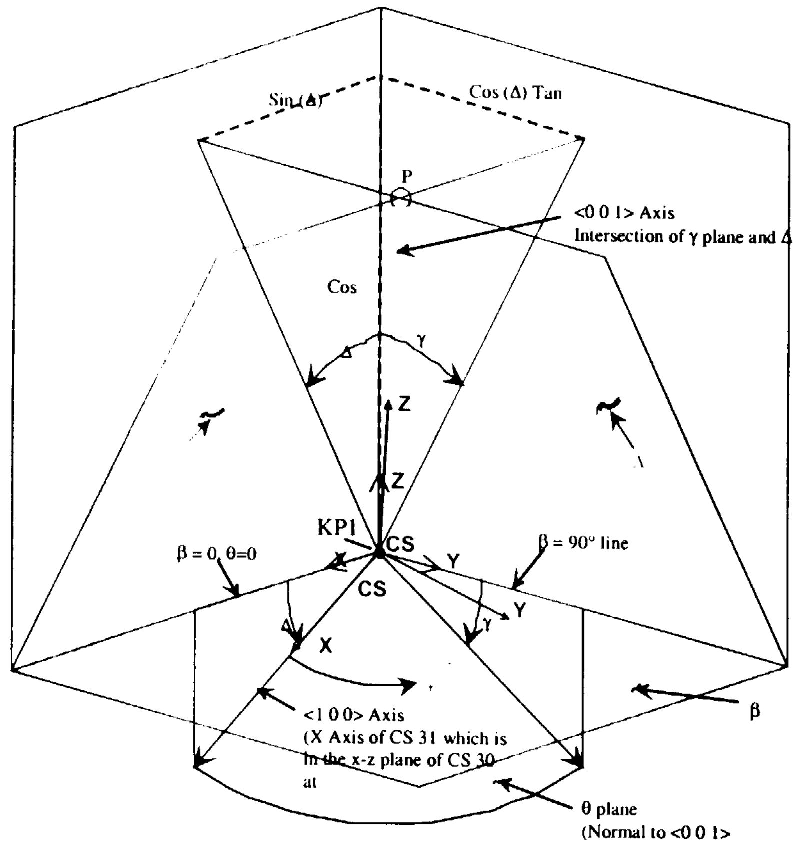

CS 30 - Blade Casting Coordinate
CS 31 - Crystallographic Coordinate system @ β=0°

Figure 5.4. First stage blade material coordinate system relative to the casting coordinate system

Fatigue Failure of Development Space Shuttle Main Engine Turbine Blades

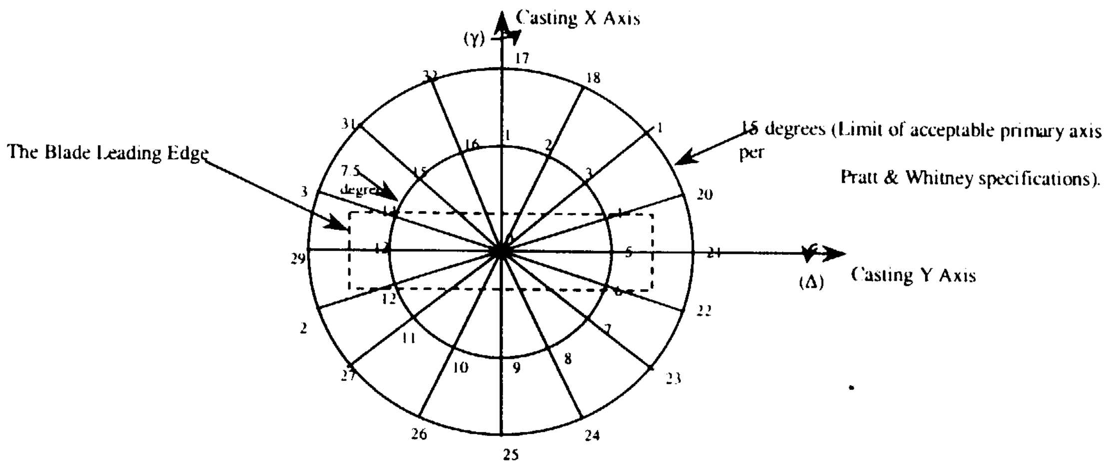

Top View of the Blade

* (33) orientations (cases) of (γ & Δ) with (9) (θ)orientations about each of these.
    * 16 cases with (γ & Δ) combined to 7.5 degrees, 16 with (γ & Δ) combined to 15 degrees, 1 case with (γ & Δ) combined to 0 degrees.
    * (θ) varied from 0 to 80 degrees in 10 degree increments about the local material axis (due to symmetry 90 degrees is the same as 0 degree).
* Total of (297) orientations.
* Angles used in the model have not been reconciled with angles reported by casting vendor.

Figure 5.5 33 primary axis cases with 9 secondary cases each, a total of 297 material orientations.

Case	Delta	Gamma	Beta
0	0.00	0.00	0,10,20,30,40,50,60,70,80
1	7.50	0.00	0,10,20,30,40,50,60,70,80
2	6.93	2.87	0,10,20,30,40,50,60,70,80
3	5.30	5.30	0,10,20,30,40,50,60,70,80
4	2.87	6.93	0,10,20,30,40,50,60,70,80
5	0.00	7.50	0,10,20,30,40,50,60,70,80
6	-2.87	6.93	0,10,20,30,40,50,60,70,80
7	-5.30	5.30	0,10,20,30,40,50,60,70,80
8	-6.93	2.87	0,10,20,30,40,50,60,70,80
9	-7.50	0.00	0,10,20,30,40,50,60,70,80
10	-6.93	-2.87	0,10,20,30,40,50,60,70,80
11	-5.30	-5.30	0,10,20,30,40,50,60,70,80
12	-2.87	-6.93	0,10,20,30,40,50,60,70,80
13	0.00	-7.50	0,10,20,30,40,50,60,70,80
14	2.87	-6.93	0,10,20,30,40,50,60,70,80
15	5.30	-5.30	0,10,20,30,40,50,60,70,80
16	6.93	-2.87	0,10,20,30,40,50,60,70,80
17	15.00	0.00	0,10,20,30,40,50,60,70,80
18	13.86	5.74	0,10,20,30,40,50,60,70,80
19	10.61	10.61	0,10,20,30,40,50,60,70,80
20	5.74	13.86	0,10,20,30,40,50,60,70,80
21	0.00	15.00	0,10,20,30,40,50,60,70,80
22	-5.74	13.86	0,10,20,30,40,50,60,70,80
23	-10.61	10.61	0,10,20,30,40,50,60,70,80
24	-13.86	5.74	0,10,20,30,40,50,60,70,80
25	-15.00	0.00	0,10,20,30,40,50,60,70,80
26	-13.86	-5.74	0,10,20,30,40,50,60,70,80
27	-10.61	-10.61	0,10,20,30,40,50,60,70,80
28	-5.74	-13.86	0,10,20,30,40,50,60,70,80
29	0.00	-15.00	0,10,20,30,40,50,60,70,80
30	5.74	-13.86	0,10,20,30,40,50,60,70,80
31	10.61	-10.61	0,10,20,30,40,50,60,70,80
32	13.86	-5.74	0,10,20,30,40,50,60,70,80

Table 5.1 33 primary axis cases with 9 secondary cases each, a total of 297 material orientations.

Fatigue Failure of Development Space Shuttle Main Engine Turbine Blades

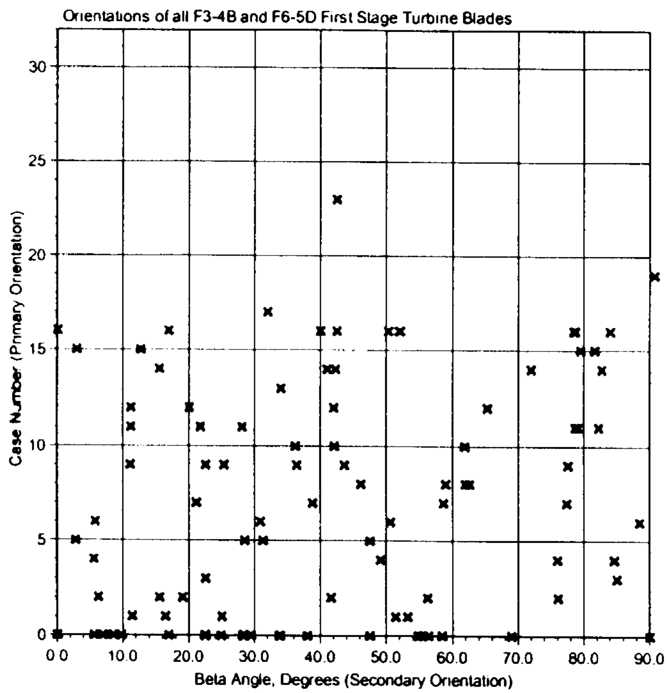

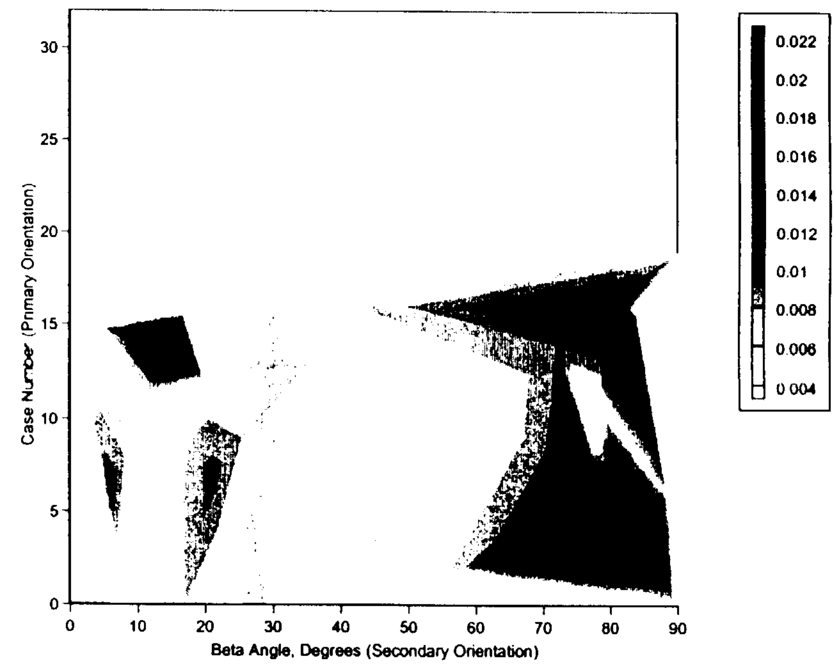

F3-4B and F6-5D First blades XXX FPI data, Contour Plot of Crack Length Across Blade Wall in Inches (0.02 is through wall for this plot)

Fatigue Failure of Development Space Shuttle Main Engine Turbine Blades

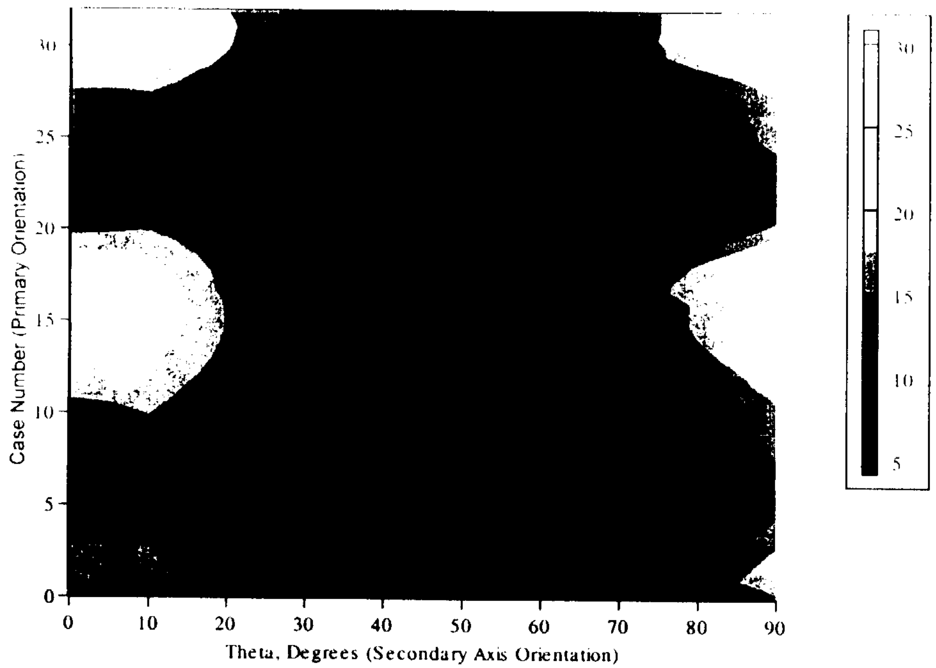

Maximum Resolved Shear Stress at Blade Tip

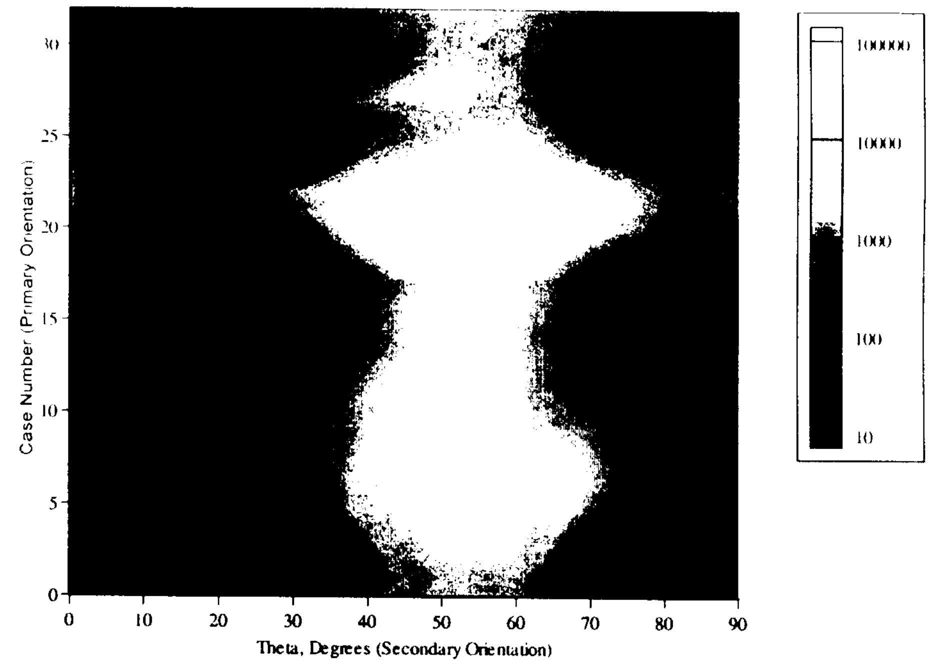

Dimensionless life at the first blade airfoil crack initiation point.

Final Comments

- **HPFTP/AT is certified for flight**
  - Development problems resolved before certification and flight
  - Final design has completed extensive hot fire testing
- **Further Development of Analytical Tools for Single Crystal Materials**
  - Currently in work
  - Needed as part of effort to further enhance blade and vane life
- **Further Development of Crystallographic Crack Growth Specimens**
  - Currently in work
  - Needed for determining the crack growth threshold for this material in the H_2 + Steam environment
- **Reference**
  - Swanson, G. R. and Arakere, N. K., "Effect of Crystal Orientation on Analysis of Single-Crystal, Nickel-Based Turbine Blade Superalloys", NASA/TP-2000-210074.